Splash Distribution in Oxygen Steelmaking

SHABNAM SABAH and GEOFFREY BROOKS

The study of splashing is important in understanding oxygen steelmaking. Splashing creates large interfacial area between reacting surfaces and thereby directly affects the kinetics of steelmaking reactions. In the present cold modeling work, a study of splashing has been carried out for various lance heights and gas flow rates. Sampling of droplets has been done in both radial positions and vertical positions across the bath to investigate the effect of sampling positions in estimation of the droplet generation rate. A novel approach has been developed to estimate the droplet generation rate. The results of the study have been compared with previous investigations. Results show that positioning of sampling is a critical issue and can affect the estimation of droplets present in the emulsion. This study also demonstrates quantitatively how much the droplet generation rate is reduced when the cavity mode changes from splashing to penetrating for different Blowing numbers.

I. INTRODUCTION

IN oxygen steelmaking, understanding splashing is an essential aspect of optimizing the process. In the literature of splashing, several terms have been frequently used by researchers which need clarification for future understanding and consistency.

A. "Percentage of Total Metal in the Emulsion" and "Weight Percentage of Sample"

In the literature, the quantity of droplets has been expressed using terms such as "percentage of total metal in the emulsion" and "weight percentage (wt pct) of the sample". "Percentage of total metal in the emulsion" refers to the percentage of droplets present in the emulsion with respect to the total metal of the bath whereas "weight percentage of the sample" refers to how much of the sample was metal with respect to the total sample weight.

B. "Splashing" and "Droplet Generation"

"Splashing" and "droplet generation" are not synonyms. "Splashing" refers to the liquid projected from the bath including the material ejected from the vessel whereas "droplet generation" refers to the part of splash that ends up in the emulsion as distinct droplets.

C. "Residence Time" and "Amount of Droplets Present in Emulsion"

Droplets, created by the impact of oxygen jet, may be ejected into the emulsion. These droplets spend some time in the emulsion before they fall back to the metal bath. "Residence time" indicates the amount of time droplets spend in the emulsion. At a certain time, the amount of droplets present in the emulsion not only depends on the droplet generation rate but also the residence time of the droplets in the emulsion. The amount of droplets present in the emulsion at any time can be calculated from the following equation using the droplet generation rate and residence time[1]

$$V_\infty = R_B \tau \qquad [1]$$

Equation [1] assumes no accumulation of droplets in the emulsion. Dogan et al.[2] proposed a residence time model that predicts the variation of the residence time of metal droplets with carbon percentage. Figure 1 shows the change of residence time of 0.002 m diameter metal droplets as a function of the carbon concentration of the bath.

Various studies (cold model, hot model, and plant trials) have been carried out previously to estimate the amount of droplets present in the emulsion. Sampling techniques have been widely used to calculate droplet amount in the emulsion. In most of the cases, sampling has been carried out in one place and the quantity of droplets found has been taken as the representative of the whole emulsion. Without describing the sampling position, the plant trial of Kozakevitch[3] found that maximum 40 wt pct of the slag sample was metal. In the work of Cicutti et al.,[4] one sample was taken from the emulsion and one from the metal bath at a time by submerging a special device into the furnace. The percentage of total metal in the emulsion was not reported in the investigation. In an investigation of 230 t BOF plant measurement, Meyer et al.[5] took samples from a pan placed on the operating floor outside the tap hole. The percentage of total metal in the emulsion was reported to be a maximum of 78 pct by weight. Price[6] studied the emulsion by the "bomb" sampling method

SHABNAM SABAH, Ph.D. Student, and GEOFFREY BROOKS, Professor of Engineering, are with the Faculty of Science, Engineering and Technology, Swinburne University of Technology, Hawthorn, VIC 3122, Australia. Contact e-mail: ssabah@swin.edu.au
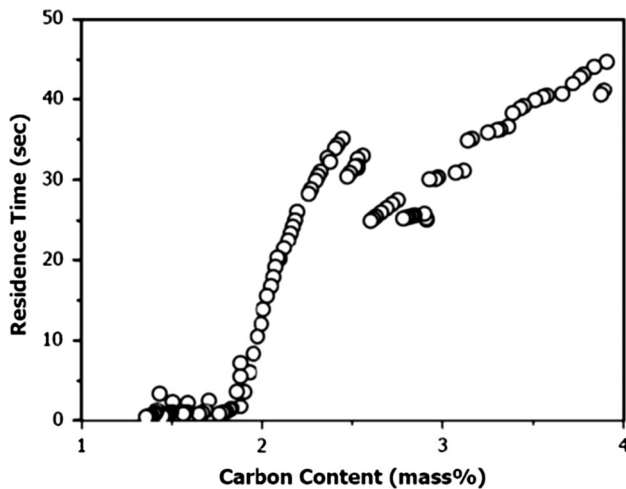
Fig. 1—Residence time vs percentage of Carbon.[2]

in 90 t BOS converter. The percentage of total metal in the emulsion was estimated to be 15 pct by weight. Schoop and his co-workers[7] also made plant measurements on a 200 t top blowing LD converter. The sampling position was not specified. The percentage of total metal in the emulsion was found to be about 1 pct by weight. Trentini[8] stated that the percentage of metal droplets from two sampling positions. When samples were taken by stopping the blow and tilting the converter, 20 wt pct of the samples was found to be metal whereas samples from the ejected slag from off the shell of converter showed 50 wt pct of the slag sample was metallic. In a 50 kg laboratory converter, Tokovoi et al.[9] took spoon samples from the upper levels of slag. Their result showed that 3 to 25 wt pct of the sample was metal. In a 1/50th scale of BOF, Urquhart and Davenport[10] took metal samples using a pin tube from the bath and a spoon of samples from the slag during the course of the blow. 26 wt pct of the sample was found to be metal. He and Standish[11,12] carried out cold model experiments with a glycerine-mercury bath, 30 wt pct of the glycerine-mercury emulsion was found to be mercury.

Urquhart and Davenport[10] used a cold temperature model (paraffin oil—4 wt pct HCO_3—in water solution) to simulate steelmaking. They found 28 wt pct of the emulsion was water. Using mercury as an analogue for the steel phase and glycerine for the slag phase, Turner and Jahanshahi[13] investigated the emulsion of metal droplets by cold model experiments. They found that 24 wt pct of the sample was mercury.

Recently, an investigation[14,15] on improving phosphorus refining (IMPHOS) commissioned by the European Union was carried out in a 6 t Pilot plant BOS converter at the Swerea MEFOS Metallurgical Research Plant in Sweden. Oxygen was blown at a constant flow rate of 17 Nm^3 min^{-1} through a single nozzle lance. The bath was agitated by a bottom single tuyere with nitrogen flow rate of 0.5 Nm^3 min^{-1}. An automated sampling system was used to collect samples from seven specified positions in every 2 min from the start of the blow. The sampling lance was kept 0.045 m offset from the center of the converter (as shown in Figure 2). The percentage of metal circulation rate (pct tap weight/second) in the emulsion phase (in three heats) varied between 7 and 13 pct by weight. In summary, the literature review shows that there is a large variation on the reported amount of droplets present in the emulsion and some confusion about how many droplets are generated and how this relates to sampling position. The present cold model study was motivated by the work of IMPHOS[15] to investigate how the amount of droplets varies depending on sampling position.

Molloy[16] identified three different cavity shapes (i.e., dimpling mode, splashing mode, and penetrating mode) for top jetting condition and stated that splashing reduced drastically when cavity mode goes into penetrating mode. There are limited studies[17] which show quantitatively how splashing behavior is affected by different cavity modes in top jetting condition. To predict droplet generation, Subagyo et al.[18] proposed a new dimensional number, called "Blowing number" (N_B) which is a ratio of inertia force to buoyancy and surface tension forces. It is defined as follows

$$N_B = \frac{\rho_g U_g^2}{2\sqrt{\sigma g \rho_l}}$$

Subagyo et al.[18] proposed an empirical formula relating metal droplet generation rate per unit volume of blown gas and N_B using their measured data of high temperature modeling and cold modeling data of He et al.[11,12] The formula is as follows,

$$\frac{R_B}{F_g} = \frac{N_B{}^{3.2}}{\left[2.6 \times 10^6 + 2.0 \times 10^{-4}(N_B)^{12}\right]^{0.2}} \quad [2]$$

This relation suggests that an increase in N_B always results into increase in the generation of droplets. But the cold modeling work of Alam et al.[17] at angled jet condition showed that splashing at high N_B was less than that of low N_B. At high N_B, the cavity mode[16] changed from splashing to penetrating and thus splashing was reduced. The study demonstrated that the Blowing number theory did not work well when cavity modes changed. The issue of how to calculate splashing in different cavity modes at top jetting condition is not clear and requires further investigation.

In the present experimental study, an approach has been taken to investigate the issue of splashing and Blowing number in different cavity modes and how sampling positions (both radial and vertical) can affect the estimation of droplets present in the emulsion under top jetting conditions.

II. EXPERIMENTAL DESCRIPTION

The present model (as shown in Figure 3) is a 1/5th model of the BOS used in IMPHOS[15] study. Compressed air and water were used to simulate oxygen and liquid steel, respectively. Compressed air was passed
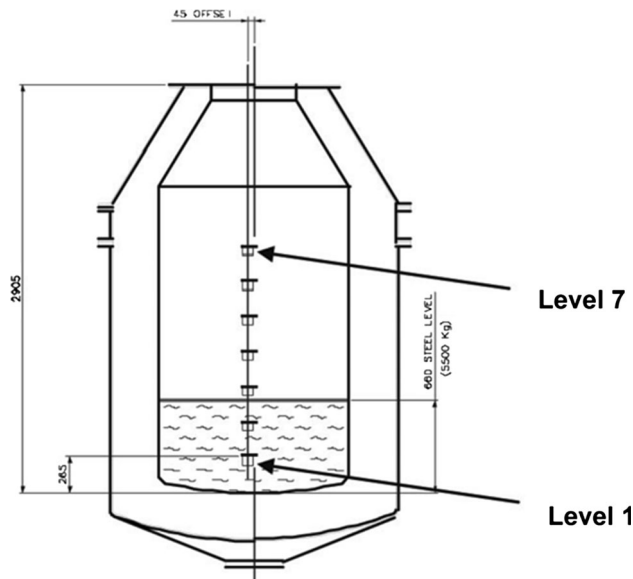
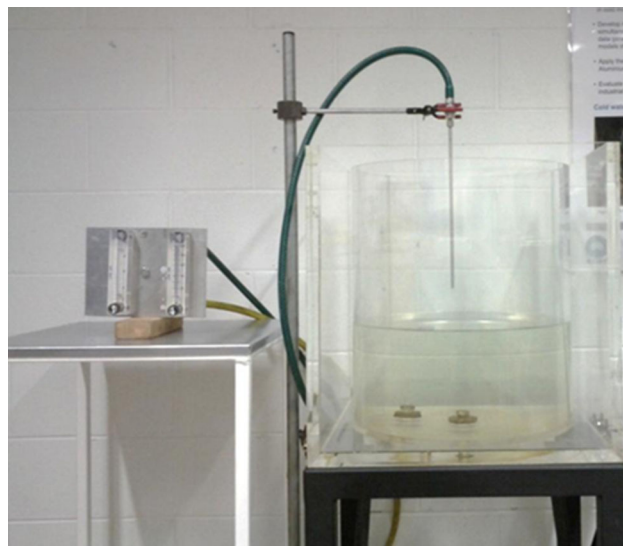Fig. 2—Schematic of IMPHOS investigation and sampling positions[14].

Fig. 3—View of experimental set-up.

Table I. Description of IMPHOS Work [15] and Present Model

Dimensions	IMPHOS BOF [15]	Present Model
Nozzle diameter, d (m)	0.0155	0.003
Vessel diameter, D (m)	1.340	0.420
Vessel height, l (m)	2.905	0.500
Bath height, H (m)	0.660	0.200
Number of nozzles, N	1	1
Lance height, L (m)	1.70, 1.60, 1.50 (heat S1845)	0.170, 0.160, 0.150 (compared with S1845), 0.120, 0.100, 0.080, 0.050 (additional)
Nozzle angle, θ (°)	0	0

and IMPHOS work. In order to cover a wide range of experimental conditions, splashing studies have been carried out at various lance heights and gas flow rates in addition to the IMPHOS conditions.

The geometric and dynamic similarity between the model and the IMPHOS converter were maintained as much as possible. The Blowing number similarity criteria were given preference as suggested by Subagyo et al.[18] The reasoning behind this has been described in detail in a different paper.[19] This, however, has increased the momentum number of the model. The similarity criteria and operating conditions are presented in the Tables II and III. A sample calculation of N_B has been presented in Appendix A for clarification. It is important to note that the values of density of air and water were taken at 273 K (0 °C) and 101325 Pa as these were the conditions that Subagyo et al.[18] used in their calculations.

A stainless steel structure was put above the cylindrical bath (as shown in Figure 4). Also, a 0.20 m stainless steel strip was perpendicularly attached to the structure. The strip was used as the sampling rod for the experiment. The strip was flexibly designed so that it could be moved along the axis of the structure. Therefore, it was possible to put the sample pots in various positions. The sample pots were cylindrical in shape with height of 0.014 m and diameter of 0.013 m. Five sample pots were attached with the strip with blue tack at a distance 0.05 m apart along the length of the strip. The positions of the pots were scaled down 1/5th from the IMPHOS investigation. For ease of identification, sample pots of IMPHOS investigation will be termed as P1, P2, P3, P4, P5, P6, and P7 (as shown in Figure 2) whereas sample pots of the present model will be labeled as M1, M2, M3, M4, M5, M6, and M7 in this paper. There were no M1 and M2 pots in this study. The sampling position of M3 was equivalent to P3; position of M4 was equivalent to P4 and so on. The position of M3, M4, M5, M6, and M7 was 0.024, 0.074, 0.124, 0.174, and 0.224 m above bath surface, respectively. Also, these sample pots were kept in various radial positions (0.033, 0.060, 0.090, 0.120, 0.150, and 0.180 m radially away from the lance) to investigate how the droplet generation rate varied radially. At a specific

through a straight nozzle. As the first phase of the study, the slag phase was not included in this work. The cold model was a transparent cylindrical rig, made of perspex sheet. The bottom surface of the rig was flat which is not in consistent with the actual steelmaking practice and therefore, it may have affected the fluid dynamics of the bath to some extent. The lance was kept at the center of the bath. In the beginning of each experiment, a laser level was used to ensure the lance was kept perpendicular to the bath. A flow meter (range: 10 to 100 L/min, accuracy ±3 pct of full scale) was used to control the flow rate of compressed air. Heat S1845 of the IMPHOS[15] investigation was taken as the target heat number to compare the results with the present work. Table I presents the details of the experimental set-up

Table II. Similarity Criteria

Dimensionless Number	Numerical Definition	IMPHOS	Present Model (Compared With Heat S1845)	Present Model (Additional Conditions)
Geometrical Similarity				
Distribution number	Nd^2/D^2	.00013	0.00005	0.00005
Bath aspect ratio	H/D	0.50	0.48	0.48
Dimensionless lance distance	L/d	97 to 110	50 to 57	16.67 to 40
Dynamic Similarity				
Blowing number (N_B)	$\frac{\rho_g U_g^2}{2 \times (\rho_l g \sigma)^{0.5}}$	2.24 to 2.53	2.37 to 2.74	1.37 to 6.71
Modified froude number	$\frac{\rho_g U_j^2}{\rho_l g L}$	0.066 to 0.084	0.38 to 0.42	0.22 to 3.20
Momentum number	$\frac{\rho_g U_0^2 d^2}{\rho_l g L^3}$	5.8×10^{-4} to 8.5×10^{-4}	8.6×10^{-3} to 9.6×10^{-3}	4.82×10^{-3} to 8.42×10^{-2}

Table III. Operating Conditions

Lance Height (m)	Compressed Air Flow Rates (L/min) (1 L/min = 1.67×10^{-5} m³/s)
0.170	60, 70, 80, 90
0.160	60, 70 80,90
0.150	55,70,80,90
0.120	50,60,70,80
0.100	50,60,70,80
0.080	35,40,50,60
0.050	30,40
Sampling positions	radial positions—0.033, 0.060, 0.090, 0.120, 0.150 and 0.180 m radially away from lance, vertical positions—0.024, 0.074, 0.124, 0.174 and 0.224 m above bath surface

Fig. 4—View of sampling rod over the bath.

radial position, droplets were collected in the vertically positioned five sample pots (M3 to M7) for duration of 3 to 150 seconds, depending on the droplet generation rate. The reason for sampling time variation was due to the size of the pots and time required to fill them. Each set of data was taken two times and an average was

determined. After each sampling process, the weights of the sample pots were measured using a digital weight scale (Model: XA204 Delta range, maximum capacity 0.220 kg). Subtracting the weight of empty pots from the measured weight, the collected droplet weight was calculated. The errors occurred in the measurement of droplets and how variations of sampling time has affected the collected droplet weight have been estimated and presented in Appendix B.

III. RESULTS AND DISCUSSION

A. Droplets Distribution in Different Sampling Positions

Droplets collected in the sample pots varied both radially and vertically across the bath. Variations in droplet amount among sample pots increased as N_B increased (i.e., momentum of gas jet on the bath increased). Here, droplet distribution at lance height (L) 0.170, 0.160, and 0.150 m at flow rate 80 L/min will be discussed in order to quantify these variations. Figure 5a shows the amount of droplets collected at various vertical and horizontal positions when the L was kept at 0.170 m and gas flow rate 80 L/min (N_B = 2.44). The sampling time was 2 minutes. It was found that the weight of the collected droplets in the pots varied significantly across the radius of the bath especially for the sample pots M3 and M4. In case of rest of the sample pots, the standard deviation of droplet weight at different radially sampling positions was found to be 0.23×10^{-3} kg only. For M3, maximum amount of droplets (i.e., $43.98 \pm 0.04 \times 10^{-3}$ kg) were found at radial distance 0.090 m from the lance. At the same radial position and sampling time, 12, 0.8, 0.6, and 0.1 pct of the droplets in M3 was found in M4 (0.074 m above the bath), M5 (0.124 m above the bath), M6 (0.174 m above bath surface), and M7 (0.224 m above bath surface), respectively.

Figure 5(b) shows the droplet distribution at L = 0.160 m and gas flow rate 80 L/min (N_B = 2.74) whereas Figure 5(c) shows droplet quantity at L = 0.150 m and gas flow rate 80 L/min (N_B = 3.10). For both operating conditions, radial position for maximum droplet collection varied from 0.060 to
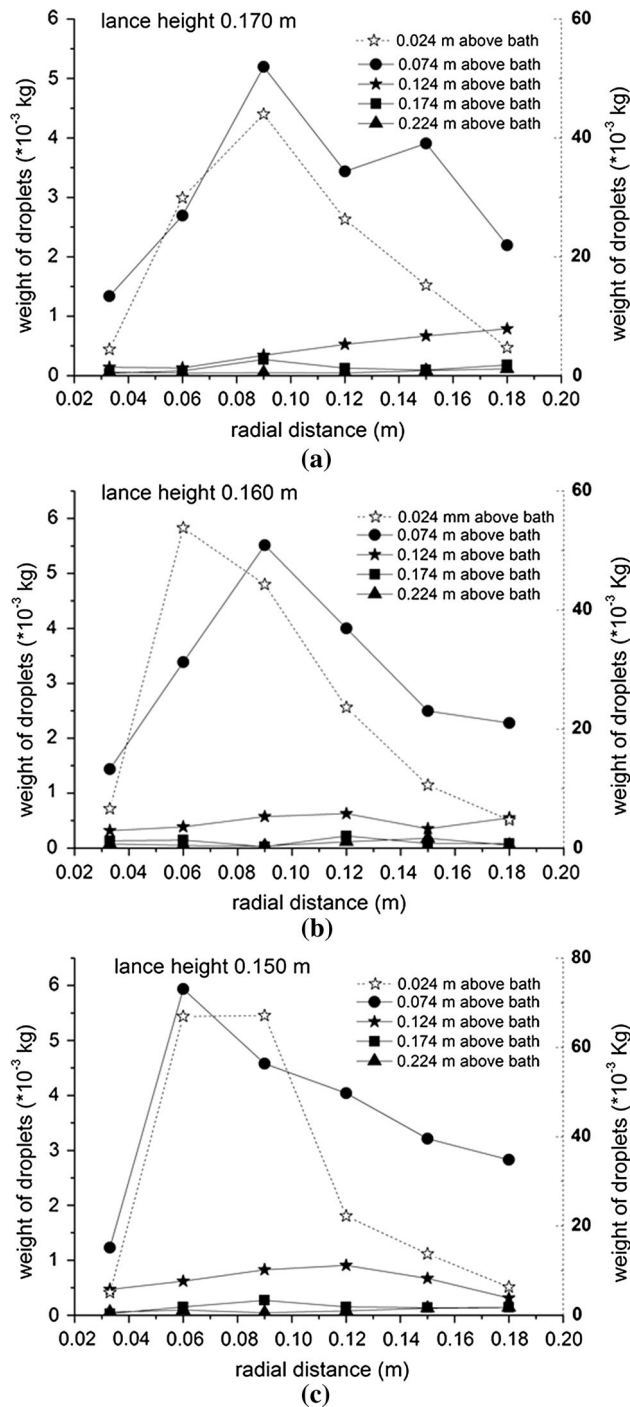
(a)

(b)

(c)

Fig. 5—(a) Droplet distribution at lance height 0.170 m; (b) Droplet distribution at lance height 0.160 m; (c) Droplet distribution at lance height 0.150 m.

0.090 m for M3 and M4. For M3, maximum droplets collected were 53.8 ($\pm$.04) $\times 10^{-3}$ kg and 67.1 ($\pm$.04) $\times 10^{-3}$ kg at $L = 0.160$ m, and $L = 0.150$ m, respectively. It implied that for M3, decreasing lance heights from 0.170 to 0.150 m increased the maximum amount of droplets collected. In case of other pots, no general trend in the amount of droplets was found for decreasing lance heights. For M5, M6, and M7, standard deviations for the amount of droplets at different
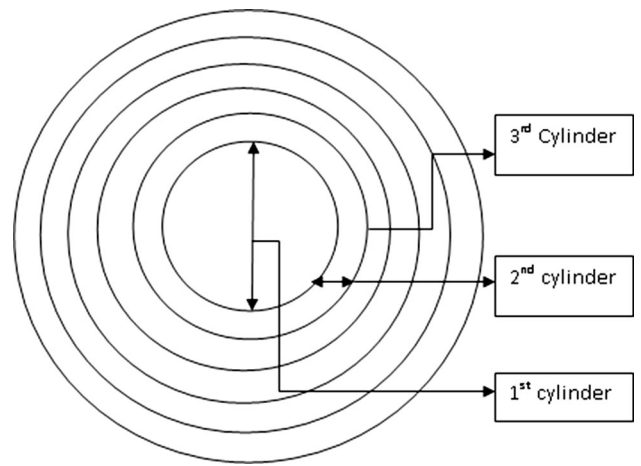

Fig. 6—An approach to calculate droplet generation rate (top view of the bath).

radial positions were calculated and it was found to be 0.20 $\times 10^{-3}$ kg (at $L = 0.160$ m) and 0.28 $\times 10^{-3}$ kg (at $L = 0.150$ m).

Therefore, it can be concluded that there were large variations in collected droplets from M3 and M4 compared with the rest of sample pots (M5 to M7). Also, noticeable radial variations in droplets were found mostly in case of samples collected from M3 and M4.

B. Rate of Droplet Generation and Sampling Positions

In order to determine the droplet generation rate at each operating condition, the bath above the water surface was divided into six cylinders (as shown in Figure 6) as there were six radial sampling positions (i.e., 0.033, 0.060, 0.090, 0.120, 0.150, and 0.180 m away from the lance). At each radial sampling position, an average of droplets collected in various vertically placed sample pots was taken as the representative of the droplet generation rate in that cylinder. The following equation was used for calculation[14]

$$\text{Droplet generation rate, } R_{\text{B}} = \frac{(\sum Wsp)V_{\text{b}}}{t_{\text{s}}V_{\text{sp}}N_{\text{sp}}} \quad [3]$$

At each operating condition, the droplet generation rate at each cylinder was calculated using Eq. [3]. Then an average of the rates was taken as the droplet generation rate at that operating condition. V_{b} is the volume of each cylinder which varied according to the radial sampling positions. A sample calculation of the droplet generation rate has been provided in Appendix A.

High speed imaging of the cavity (as shown in Figure 7(a)) has been carried out[19] which showed the generation of "splash sheets". These sheets like structures have been also described in a slag splashing study by Liow et al.[20] and in general splashing literature by Deegan et al.[21] Figure 7(b) shows a schematic representation of the cavity and splash distribution. Splash sheets were formed by the reflected gas velocity and fell into the sample pots closer to the bath (i.e., M3 and M4). For this reason, the amount of droplets collected
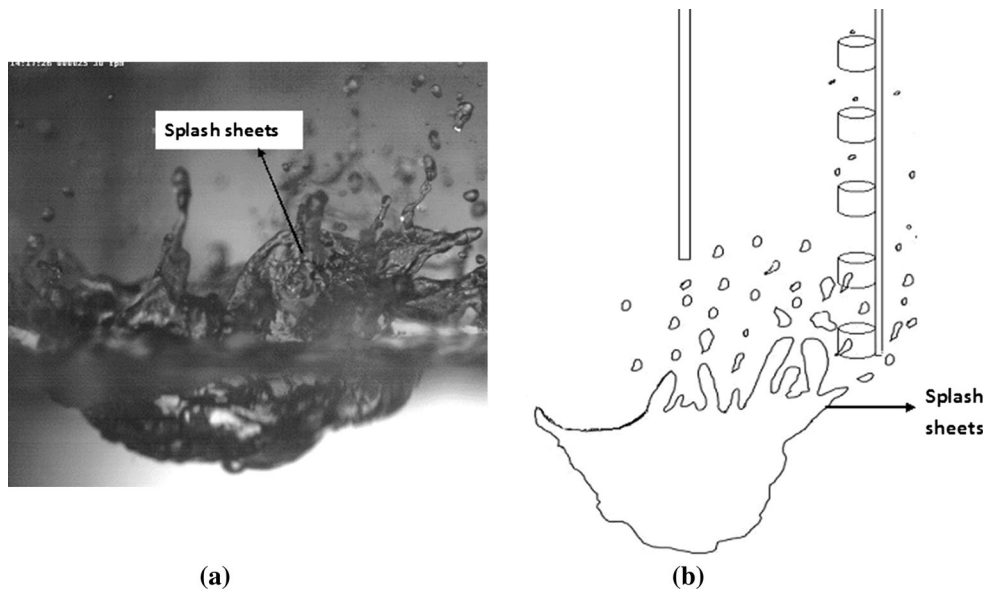
Fig. 7—(a) Formation of sheets from high speed imaging; (b) Schematic of splash distribution.

in M3 and M4 was much greater than that of other pots. Therefore, it was judged that the droplet generation rate should be calculated excluding the sample pots M3 and M4.

Milliman et al.[14] excluded P3 (which is equivalent M3 in the present work) when calculating the droplet generation rate. When calculating the droplet generation rate in the present work, droplets collected in M3 were also not considered. Figure 8 compares the rates of droplet generation at lance height 0.150 m and flow rate 80 L/min excluding only M3 and excluding both M3 and M4. When the droplets collected in both M3 and M4 (which were closest to the bath) were excluded from the rate calculation there was drastic reduction in the value of rates. For example, the maximum droplet generation rate reduced from 36.18 to 10.77 $\times$ 10^{-3} kg/s. It is important to note that, when N_B became greater than 2, large variations in droplet weights occurred among M3 and M4 with the rest of sample pots. Therefore, it was judged that the droplet generation rate should be calculated excluding M3 and M4 when N_B exceeds 2. When N_B was less than 2, droplets collected in all pots were included in the rate calculation as splash sheets formation didn't occur at those conditions.

This quantitative analysis of the droplet generation rates shows that how much sampling position affects the prediction of the droplet generation rate and sampling too close to the bath can produce overestimated results in the amount of droplets that end up in the emulsion.

C. Comparison with Previous Work

Figure 9 compares the results of the present work and Eq. [2] proposed by Subagyo et al.[18]. In the graph, the X axis represents the Blowing number (N_B) and the Y axis shows droplet generation rate in kilograms per seconds (R_B) per volumetric flow of blown gas (F_g) in normal cubic meters (101325 Pa and 273 K (0 °C)) per

second. It was suggested from Eq. [2] that with an increase in N_B, the droplet generation will also increase.

The droplet generation rate (R_B) presented in Figure 9, is an average droplet generation rate of sample pots placed in various radial positions. F_g has been converted from operating conditions to pressure 101325 Pa and temperature 273 K (0 °C) condition to be consistent with the work of Subagyo et al.[18]. Figure 9 shows that the results of present work are in good agreement with the investigations of He and Standish[11, 12] and Subagyo et al.[18]. The R_B/F_g for heat S1845 of IMPHOS was found in the range of 180 to 360 kg/Nm^3. Figure 8 shows that sampling pots which were closest to the bath (i.e., M3 and M4), collected greater amounts of droplets compared with the other sample pots due to the formation of splash sheets. Therefore, estimation of the droplet generation rate incorporating droplets found in M3 and M4 is likely to give overestimation in the droplet generation rate. As sampling positions of P3 and P4 of IMPHOS are in equivalent positions as M3 and M4, droplets collected in both P3 and P4 should be excluded from the R_B calculation in IMPHOS work. Though P3 was excluded from the calculation of IMPHOS study, present analysis showed that P4 also needed to be excluded from the droplet generation rate calculation.

D. Splashing Study and Blowing Number

Figure 10 represents the results of the present cold model study and Eq. [2] proposed by Subagyo et al.[18] It demonstrates how droplet generation rate per volumetric flow rate of blown gas (R_B/F_g) was affected by cavity modes and Blowing number (N_B). The volumetric flow rate of blown gas of operating conditions was calculated for conditions 101325 Pa pressure and 273 K (0 °C) temperature as Eq. [2] was specifically developed for these conditions[18]. Each point of the graphs presented
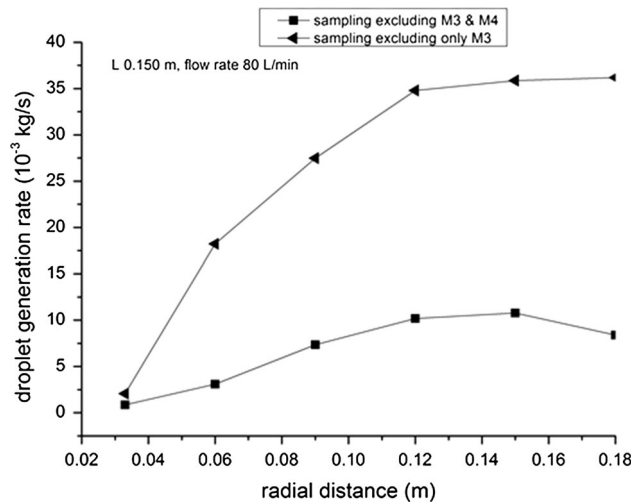
Fig. 8—Droplet generation rates in different radial positions.

in Figure 10 was acquired from an average of 25 different sampling places across the bath. Also, each experiment was carried out 2 times for better estimation of the values.

Results showed that R_B/F_g was dependent on the lance heights. At a constant lance height, with increasing of N_B, the droplet generation rate per volume flow rate of blown gas increased in general. At higher lance heights of 0.170, 0.160, and 0.150 m, R_B/F_g was greater than that of lower lance heights (from 0.120 m to downwards). When the lance height was lowered to 0.120 m, there was drastic reduction in the value of R_B/F_g. From the lance height 0.120 to 0.050 m, the values of R_B/F_g were found to be lowest. This was so because the cavity mode entered into penetrating mode from splashing mode when the lance height was lowered to 0.120 m. High speed imaging of the cavity[19] showed that the height of splash sheet decreased when the cavity went into penetrating mode, and therefore, the droplet generation rate per volumetric flow of blown gas also reduced.

The results of present work were also compared with Eq. [2] given by Subagyo et al.[18] The equation was developed for a fixed lance height. Present results consisted of various lance heights. Also, there were unavoidable experimental errors associated with the present experiment which is important to acknowledge. The errors associated with the measurement of droplet weight and how variations of sampling time have affected the collected droplet weight is presented in Appendix B. Droplets hitting the wall of sample pots were not included in this study. Only the droplets entering the sample pots were used in the droplet generation rate calculation. Therefore, this study under predicts the droplet generation rate. Trajectories of the droplets were also affected by the existence of sampling rod and sample pots. Some of the droplets hitting the sample rod may have been collected into the sample pots. In addition, for calculation of the droplet generation rate at a particular operating condition, averaging of droplet generation rate in different radial positions
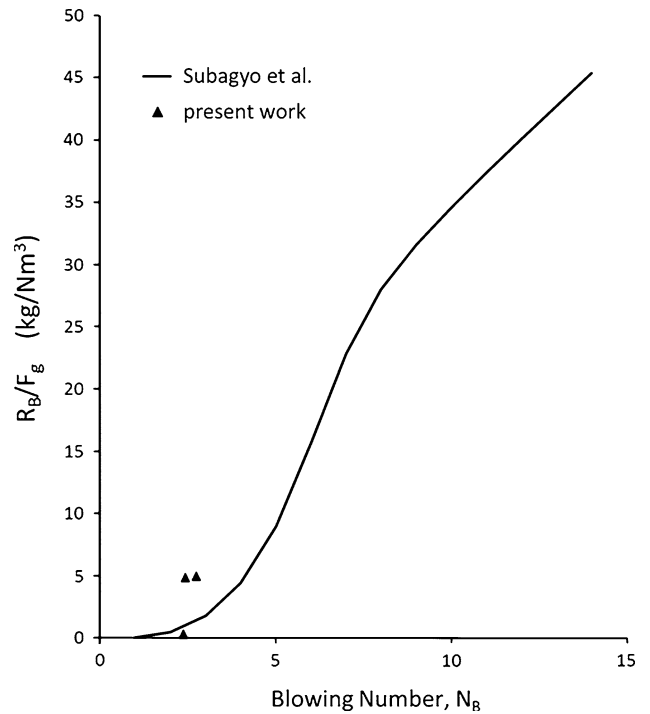

Fig. 9—N_B vs droplet generation rate (R_B) per volumetric flow of blown gas.

was carried out. Therefore, variations could be expected between the results of the present work and Subagyo et al.[18]

Despite the errors that may have been induced in estimation of droplets in the experiments, Figure 10 showed quite distinctively how the droplet generation rate was affected by the occurrence of cavity modes and why it is important to identify various cavity modes in the study of steelmaking. In Figure 10, at $N_B = 3$, R_B/F_g was found to be dependent on the cavity mode. If the cavity was in splashing mode (i.e., at higher lance heights), the R_B/F_g was found to be in the range of 5 to 9 kg/Nm^3(approx.). On the other hand, R_B/F_g became 0.4 kg/Nm^3 (approx.) when the cavity entered into penetrating mode (i.e., at lower lance heights) at the same Blowing number. It means that higher N_B does not necessarily indicate higher droplet generation rate. N_B along with cavity mode is needed in estimating droplets amount. Alam et al.[17] carried out a small-scale thin slice model experiment in an angled jet condition. The results of their work showed that at higher N_B with the cavity in the penetrating mode, the droplet generation rate was lower than that of lower N_B with the cavity in splashing mode. Present results displayed similar findings though jetting conditions were not the same in both studies.

In order to provide a relation between R_B/F_g and N_B in splashing mode, an empirical relation has been proposed from the results of present cold modeling experiment. The former one proposed by Subagyo et al.[18] was based on constant lance height. Therefore, the current relation with various lance heights is meant to provide a better prediction for the droplet generation
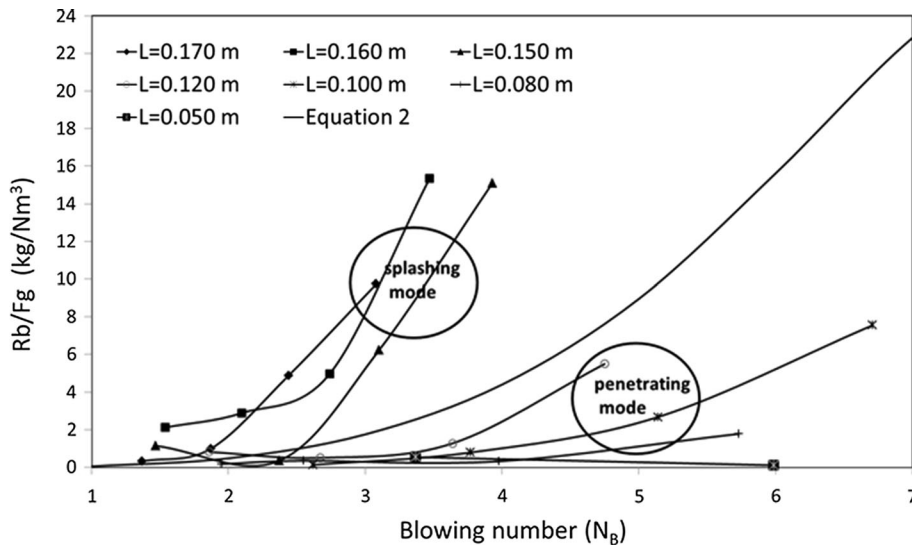
Fig. 10—Blowing Number (N_B) *vs* droplet generation rate per volumetric flow rate (R_B/F_g) of blown gas.

rate. Using best fit curve method, the following equation was derived

For splashing mode (when $L/d \geq 50$)

$$\frac{R_B}{F_g} = -0.8819N_B^4 + 7.4932N_B^3 - 18.567N_B^2 + 14.766N_B$$

The relation provides a reasonable fit (R squared value = 0.9087). It is only valid for $1.5 \leq N_B \leq 4.0$ as it has been developed from this range of blowing numbers only. From this work, it was found that splashing mode occurred when $L/d \geq 50$. On the other hand, penetrating mode occurred when $L/d \leq 40$ and $1.86 \leq N_B \leq 6.71$. This behavior requires further investigation. It was not possible to propose any empirical relation for penetrating mode due to the scattered data points. It was interesting to note that R_B/F_g in penetrating mode was found to be lower than predicted by Eq. [2] proposed by Subagyo et al.,[18] as can be seen in Figure 10.

The results showing the effect of sampling positions from the cold model study is quite important for plant trials or hot model experiments to avoid overestimation or underestimation in the amount of droplets in the emulsion. Also, the empirical relationship proposed in the paper is expected to provide better estimation of the droplet generation rate in splashing mode.

In practical steelmaking process, blowing of oxygen in higher and lower lance heights are termed as "soft" and "hard" blowing, respectively. From the present results, it is predicted that when blowing of oxygen goes from "soft" blowing to "hard" blowing, droplet generation rates begin to rise. As the lance gets closer to the bath during hard blowing, there is a certain point beyond which droplet generation decreases with decreasing lance height. In every industrial converter, in the hard blowing condition, we postulate that there is a certain lance height after which the droplet generation rate decreases and penetrating effect sets in. When droplet generation is the main concern, working in splashing

mode is recommended whereas it may be advantageous to operate in penetrating mode when steelmakers are trying to avoid slopping by lowering gas generation, as fewer droplets will lead to lower decarburization and lower gas generation. During steelmaking, many chemical reactions take place. From the present one-phase cold modeling study, it is not possible to predict how different elements in the hot metal affect slag formation and how this is connected to penetrating and splashing behavior. Further work is required to link slag generation and splashing behavior.

In summary, a splashing study has been carried out looking at the effect of splashing mode and sampling position on predicting droplet generation. There is a key requirement to link these findings to industrial practice through plant trials and also to develop an energy balance for the injection process. These are topics currently been investigated by this research group.

IV. CONCLUSIONS

In the present cold modeling work, a sampling technique has been used to estimate how sampling position affected the amount of droplets collected in sample pots. Sampling has been carried out for both vertical and radial positions across the bath. The following findings can be concluded from the investigations

1. There are large variations in the collected droplet amount among the sample pots. Specially, the sample pots which were closest to the bath collected more droplets than that of the other sample pots.
2. Across the radial sampling positions, variations were greatest only for the pots close to the bath.
3. The sample pots furthest from the bath collected the lowest amounts of droplets.
4. When $N_B > 2$, sheet like structures were found to form which resulted into the higher droplet count in the sample pots closest to the bath.

5. At a constant lance height, with increasing N_B, droplet generation always increased.
6. At a constant Blowing number, droplet generation rate per volumetric flow rate of blown gas decreased drastically as the cavity mode changed from splashing to penetrating. These findings indicate that Blowing number and the cavity mode are required to estimate the droplet generation rate.
7. Results of the current study showed quantitatively how the droplet generation rate was affected by the cavity modes in oxygen steelmaking.
8. An empirical relation has been proposed to relate R_B/F_g and Blowing number in splashing mode.

APPENDIX A

Blowing Number Sample Calculation

Flow rate, Q (L/min) = 80;
Lance height, L (m) = 0.170;
Density of air at 273 K (0 °C) and 101325 Pa, ρ_g (kg/m^3) = 1.29;
Nozzle diameter, d (m) = 0.003;
Density of water at 273 K (0 °C) and 101325 Pa, ρ_l (kg/m^3) = 999.84;
Radius of the nozzle, r (m) = $(d/2)$ = (0.003/2) = 0.0015;
Velocity at nozzle exit, $U_0 = \frac{Q}{\frac{\pi}{4}d^2} = \frac{\frac{80}{1000 \times 60}}{\frac{\pi}{4} \times (.003)^2} = 188.63$ m/s

Impact velocity at bath surface[12]

$$U_j = U_0 \frac{0.97}{\frac{aL}{r} + 0.29}$$

or, $U_j = 188.63 \times \frac{0.97}{\frac{0.07 \times 0.170}{0.0015} + 0.29} = 22.25$ m/s

(Subagyo *et al.*[18] used the value of a = 0.07 for cold model experiments, 0.0382 for hot model data with no gas–metal reaction and 0.0393 for plant data with gas–metal reaction)

Critical gas velocity, $U_g = \eta U_j = 0.44721 \times 22.25 = 9.95$ (η = constant = 0.44721)
Blowing Number, N_B

$$N_B = \frac{\rho_g U_g^2}{2\sqrt{\sigma \rho_l g}} = \frac{1.29 \times (9.95)^2}{2 \times \sqrt{0.07 \times 9.81 \times 999.84}} = 2.44$$

Droplet Generation Rate Sample Calculation

At lance height, L = 0.170 m, flow rate 80 L/min
Droplet generation rate calculation for cylinder 3,
Amount of droplet collected (M5 to M7), W_{sp} = 0.056 × 10^{-3} kg
Sampling time, t_s = 10 seconds
No of sample pots, N_{sp} = 3

Volume of the sample pots, V_{sp} = π × (0.0065)^2 × 0.014 = 0.000001858 m^3
Volume of the third cylinder, V_b = π × (0.09^2 − 0.06^2) × 0.303 = 0.00428436 m^3

Droplet generation rate, R_B

$$= \frac{(\sum Wsp)V_b}{t_s V_{sp} N_{sp}} = \frac{0.056 \times 10^{-3} \times 0.00428436}{10 \times 0.000001858 \times 3}$$
$$= 4.30 \times 10^{-3} \text{kg/s}$$

APPENDIX B

Error in Measurement of Weight of Droplets

At a particular operating condition and sampling place, droplets were collected twice and an average was taken. In estimation of the error, the variation of the weight of droplets collected with the number of experiments was analyzed.
For flow rate 80 L/min, lance height 0.160 m
Standard deviation of droplets weight (for 20 experiments), $S \approx \sigma$ = 0.083 × 10^{-3} kg
Confidence level 95 pct (level of significance, α = .05)
z = 1.96 (at $1 - \alpha/2 = 1 - 0.05/2 = 0.9750$)

Margin of error, $ME = \sqrt{\frac{z^2\sigma^2}{n}} = \sqrt{\frac{1.96^2 \times 0.000083^2}{20}} = 0.04 \times 10^{-3}$kg
It means that we are 95 pct confident that error in estimating the mean of droplet weight is no more than ±0.04 × 10^{-3} kg.

Error Due to Sampling Time Variation

Sampling time has varied from 3 to 150 seconds in different operating conditions. In this error estimation, it has been investigated how weight of droplets was affected by the sampling time variation.
For sample pot 2, L = 0.160 m, flow rate 80 L/min
Weight of droplets (sampling time 10 seconds) = 0.3332 × 10^{-3} kg
Weight of droplets (sampling time 5 seconds) = 0.18248 × 10^{-3} kg
Weight of droplets for 10 s = $(0.18248 \times 10^{-3}/5) \times 10 = 0.36496 \times 10^{-3}$kg
Error for sample time variation (between sampling time 5 and 10 seconds) = [(0.36496 − 0.3332)/0.3332] × 100pct = 9.53pct
Weight of droplets (sampling time 20 seconds) = 0.73966 × 10^{-3} kg
Weight of droplets for 10 s = (0.73966/20) × 10 = 0.36983 × 10^{-3}kg
Error for sample time variation (between sampling time 20 and 10 seconds)

$$= [(0.36983 − 0.3332)/0.3332] \times 100\text{pct} = 10.99\text{pct}$$

NOMENCLATURE

d	Nozzle diameter (m)
r	Nozzle radius (m)
D	Vessel diameter (m)
l	Vessel height (m)
H	Bath height (m)
L	Lance height (m)
N	Number of nozzles (−)
θ	Nozzle angle (°)
ρ_g	Density of gas at pressure 101325 Pa and temperature 273 K (0 °C) (kg/m³)
ρ_l	Density of liquid at pressure 101325 Pa and temperature 273 K (0 °C) (kg/m³)
U_g	Critical gas velocity (m/s)
U_0	Gas velocity at nozzle exit (m/s)
U_j	Gas velocity at bath surface (m/s)
g	Gravitational acceleration (m/s²)
σ	Surface tension (N/m)
N_B	Blowing number (−)
Q	Gas flow rate at nozzle exit (L/min)
η	Constant (−)
W_{sp}	Weight of droplets collected in different pots (kg)
t_s	Sampling time (seconds)
N_{sp}	Number of sample pots (−)
V_{sp}	Volume of a sample pot (m³)
V_b	Volume of each cylinder above the bath (m³)
R_B	Droplet generation rate (kg/s)
F_g	Volume of blown gas (Nm³/s)
R_B/F_g	Droplet generation rate per unit volume of blown gas (kg/Nm³)
τ	Residence time (s)
V_∞	Weight of droplets after reaching steady state (kg)
α	Level of significance (−)
S	Standard deviation of samples (−)
σ_p	Standard deviation of population (−)
z	Standard score (−)
ME	Margin of error (kg)

REFERENCES

1. Subagyo, G.A. Brooks and K.S. Coley: *Ironmak. Conf. Proc.*, 2002, pp 749–762.
2. N. Dogan, G.A. Brooks, and M.A. Rhamdhani: *ISIJ Int.*, 2011, vol. 51, pp. 1093–101.
3. P. Kozakevitch: *J. Met.*, 1969, vol. 21, pp. 57–68.
4. C. Cicutti, M. Valdez, T. Pérez, J. Petroni, A. Gómez, R. Donayo, and L. Ferro: *6th Int. Conf. Molten Slags, Fluxes Salts*, 2000, p. 367.
5. H. Meyer, W. Porter, G. Smith, and J. Szekely: *J. Met.*, 1968, vol. 20, pp. 35–42.
6. D. Price: *Process Eng. Pyrometall. Symp.*, 1974, pp. 8–15.
7. J. Schoop, W. Resch, and G. Mahn: *Ironmak. Steelmak.*, 1978, vol. 22, pp. 72–79.
8. B. Trentini: *Trans. TMS-AIME*, 1968, vol. 242, pp. 2377–88.
9. O. Tokovoi, A. Stroganov, and D. Povolotsky: *Steel USSR*, 1972, vol. 2, pp. 116–17.
10. R. Urquhart and W. Davenport: *Can. Metall. Q.*, 1973, vol. 12, pp. 507–16.
11. N. Standish and Q.L. He: *ISIJ Int.*, 1989, vol. 29, pp. 455–61.
12. Q.L. He and N. Standish: *ISIJ Int.*, 1990, vol. 30, pp. 305–09.
13. G. Turner and S. Jahanshahi: *Trans. Iron Steel Inst. Jpn.*, 1987, vol. 27, pp. 734–39.
14. M. Millman, A. Overbosch, A. Kapilashrami, D. Malmberg, and M. Brämming: *Ironmak. Steelmak.*, 2011, vol. 38, pp. 499–509.
15. M.S. Millman, A. Kapilashrami, M. Bramming, and D. Malmberg: *Imphos: Improving Phosphorus Refining*, Publications Office of the European Union, Luxembourg, 2011.
16. N. Molloy: *J. Iron Steel Inst.*, 1970, vol. 216, pp. 943–950.
17. M. Alam, G. Irons, G. Brooks, A. Fontana, and J. Naser: *ISIJ Int.*, 2011, vol. 51, pp. 1439–47.
18. Subagyo, G.A. Brooks, K.S. Coley, and G.A. Irons: *ISIJ Int.*, 2003, vol. 43, pp. 983–89.
19. S. Sabah and G. Brooks: *ISIJ Int.*, 2014, vol. 4, pp. 836–44.
20. J.L. Liow and N.B. Gray: *Metall. Mater. Trans. B*, 1996, vol. 27B, pp. 633–46.
21. R. Deegan, P. Brunet, and J. Eggers: *Nonlinearity*, 2008, vol. 21, pp. c1–c11.